Hole dynamics in the t-J model: An exact diagonalization study

Y. Hasegawa* and D. Poilblanc
Theoretische Physik, Eidgenössische Technische Hochschule Hönggerberg, CH-8093 Zürich, Switzerland
(Received 18 April 1989)

Exact many-body states of square clusters up to 18 sites (with periodic boundary conditions) are investigated in order to study the dynamics of one or two holes in the t-J model. Our method takes full advantage of the translation, rotation, and reflection symmetries of the cluster. Using a modified Lanczos algorithm, we calculate the lowest state of all the different space-group representations and its total spin as well as its spin and hole correlations. For a single hole, at intermediate J/t values, the magnetic, kinetic energies, and staggered magnetization follow J/t power-law behaviors with size-dependent exponents. A binding energy of order J between two holes appears for sufficiently large J/t (≥ 0.25). One-hole and two-hole calculations give different results regarding the stability of the Nagaoka state (against the singlet state) when $J/t \to 0$. Energy expectation values of variational resonating-valence-bond states are calculated exactly and optimized. Significant overlaps with the exact states are found for any symmetry.

I. INTRODUCTION

The recent discovery of the high-T_c copper oxide superconductors[1] has caused renewed interest in the properties of strongly correlated electrons. The two-band Hubbard model is the simplest model to describe the CuO_2 planes with d states on the Cu atoms and p states on the O atoms. However it can be reduced in certain limits to a simpler effective two-dimensional one-band Hamiltonian H of the t-J form,[2]

$$H = -t \sum_{\langle i,j\rangle,\sigma} (a_{i\sigma}^{\dagger} a_{j\sigma} + a_{j\sigma}^{\dagger} a_{i\sigma}) + \sum_{\langle i,j\rangle} J(\mathbf{S}_i \cdot \mathbf{S}_j - \tfrac{1}{4} n_i n_j) , \quad (1)$$

where $a_{i\sigma}^{\dagger} = (1 - n_{i,-\sigma}) c_{i\sigma}^{\dagger}$ and $n_i = \sum_{\sigma} c_{i\sigma}^{\dagger} c_{i\sigma}$. $c_{i\sigma}^{\dagger}$ creates an electron of spin σ on site i. The constraint of no doubly occupied site is ensured by the definition of the $a_{i\sigma}^{\dagger}$ fermion operators. The parameters t and J which describe the hopping matrix element for the charged singlet and the Heisenberg coupling between nearest neighbors (NN's) are to be determined from experiment. Even the large-U limit of the single-band Hubbard model can be written in the form (1) when the hole density is small; in this case $J = 4t^2/U$ and terms of higher order in t/U are neglected as well as the three-sites term of order Jn_h.

In the past year there has been a lot of work on mean-field approximations to H. The problem of handling the local constraint on H, which limits the occupation on any site to at most one electron, is difficult and can only be approximately treated for an infinite system. The other alternative is to solve exactly this problem but on a finite-size cluster. For the undoped system (Heisenberg), it is well established that the ground state is a singlet state which becomes degenerate with the lowest triplet state in the thermodynamic limit.[3] This leads to a finite staggered magnetization of the order of 60% of the classical Néel state. Monte Carlo simulations have led to similar conclusions.[4] In the doped case, except in the Nagaoka limit ($J = 0$, infinitely small doping), the situation is far from clear. A disordered spin liquid state was proposed to be stabilized by doping versus the antiferromagnetic (AF) long-range order. Exact calculations are then expected to give useful information on both the ground state[5–7] (GS) and the spin liquid properties.[8,9]

We report here exact diagonalizations of (1) on $L = 10$-, 16-, and 18-site clusters for one hole and $L = 10$- and 16-site clusters for two holes. We have recovered many of the results of Ref. 6 but we still have some discrepancies on a few points. This may come from the fact that a different method has been used in Ref. 6 where the Hilbert space of the 4×4 Hamiltonian is generated by tensorial product of the Hilbert space of the 2×2 Hamiltonian. Therefor it is not clear to us to which extent the Q vector of the GS can be controlled in Ref. 6. In this sense, we think our method can give more accurate informations on the physics of Hamiltonian (1).

II. EXACT DIAGONALIZATIONS

A. Lanczos algorithm

The Hamiltonian (1) is invariant under spin rotation, so we have restricted ourselves to the subspace of minimum total S_z, i.e., $S_z = 1/2$ for one hole and $S_z = 0$ for two holes. Indeed the $2S + 1$ multiplet of a given spin S state can be obtained easily from the single state of minimum S_z by rotation in spin space. Furthermore, on a finite-size cluster with periodic boundary conditions one can use the translation symmetries to reduce the dimension of the Hilbert space. The way the states transform under translation is characterized by a wave vector in reciprocal space. The maximum size of the Hilbert space we have considered was then reduced to 25 740 ($L = 16$, two holes). Finally we have used the rotations around one lattice point and (except for the 10-sites clus-

ter) the reflections. For each **k** point in the Brillouin zone we have considered the irreducible representations of the point group operations which keep this **k** point invariant. Depending on the **k** point considered, this group may contain only the identity or possibly also the well known C_4, C_{4v}, C_{2v}, and C_s point groups which have 3, 5, 4, and 2 irreducible representations, respectively, labeled by A_1, A_2, etc.

The lowest state in every subspace is found by using a modified Lanczos method. Let us sketch briefly the algorithm.[10] One starts with a trial state $|\Psi_0\rangle$ on which one applies the Hamiltonian (1),

$$H|\Psi_0\rangle=\varepsilon_0|\Psi_0\rangle+\beta|\Psi_1\rangle \ , \tag{2}$$

where Ψ_1 is a state orthogonal to Ψ_0. One cen then minimize the energy expectation value by linearly combining $|\Psi_0\rangle$ and $|\Psi_1\rangle$. This is simply achieved by diagonalizing the 2×2 matrix

$$\begin{bmatrix} \varepsilon_0 & \beta \\ \beta & \varepsilon_1 \end{bmatrix} , \tag{3}$$

where $\varepsilon_1=\langle\Psi_1|H|\Psi_1\rangle$. It is understood that no Hamiltonian symmetry breaking can appear in a finite system, so that the initial state $|\Psi_0\rangle$ can be chosen with all the symmetries previously mentioned. The Lanczos step is then iterated until convergence is obtained. At each step the Hamiltonian is applied twice and the symmetries of the initial state are preserved.

B. One-hole GS properties

We have studied one hole on 10-, 16-, and 18-site clusters for $0\le J/t\le\infty$. The region $J/t\ll1$ corresponds to the strong correlation limit of the Hubbard model although large J/t would describe a nearly static hole (or impurity) with a large effective mass. The energy values for $J/t=0.25$ for all space-group symmetries are shown in Tables I–III. The exact symmetries of the ground state have some common features in these data; indeed the GS has a total spin $\frac{1}{2}$ (its smallest value) and its wave vector lies in the pseudo-Fermi surface (FS) or is one of the closest wave vectors to the FS allowed by the periodicity of the cluster. Furthermore, in all cases, the GS belongs to the A_1 representation, i.e., they are completely symmetric with respect to all the point group operations which leave the **Q** vector invariant.

It should be noted that for $L=16$ the GS are sixfold degenerate at wave vectors $(\pm\pi/2,\pm\pi/2)$, $(\pi,0)$ and $(0,\pi)$. This is related to an additional symmetry appearing only in the 4×4 cluster; the latter can be mapped onto the $2\times2\times2\times2$ hypercube where the exchange of any pair of coordinates is a symmetry of the Hamiltonian (1) (i.e., it conserves the NN distances). This extra symmetry is also responsible for the degeneracy of the $(\mathbf{Q}=0,B_1)$ and the $(\mathbf{Q}=(\pi,0),B_1)$ excited states, where B_1 corresponds to antisymmetric states under $\pi/2$ rotation (π rotation) for $\mathbf{Q}=0$ [$\mathbf{Q}=(\pi,0)$]. The $L=10$ cluster has also a similar specific symmetry which we shall discuss later in analyzing the two-hole results.

These GS characteristics are still valid on a wide range of the parameter J/t down to a critical value $(J/t)_1\sim0.15$, 0.075, and 0–0.1 for $L=10$, 16, and 18, respectively. Below this critical value there is an abrupt transition, due to the Nagaoka effect, to a uniform ($\mathbf{Q}=0$) ferromagnetic state ($S=S_{\max}$) of the same A_1 symmetry. The energy dependence versus J/t is plotted on Fig. 1 (for $L=16$).

Above $(J/t)_1$, if the periodic boundary conditions do not allow any **k** point on the FS ($L=10,18$), the GS wave vector depends on J/t (although it is always close to the FS). Let us consider $L=10$; above $(J/t)_2=0.27$ it is *inside* the FS as in the noninteracting Fermi sea and *outside* for lower values in agreement with recent work by Ogata and Shiba.[11] When $(J/t)_1\le J/t\lesssim(J/t)_2$, the eight wave vectors close to the FS are nearly degenerate, the energy difference being smaller than $J/15$, much smaller than the total bandwidth (of order J). This indicates that the strong correlations lead to nontrivial effects com-

TABLE I. Energies and spins of the one-hole exact states classified according to their symmetries for $L=10$ and $J/t=0.25$.

		A_1	B_1	E
	E_1-E_0	−1.423	−1.457	−1.310
$\mathbf{Q}=(0,0)$	spin	$\frac{1}{2}$	$\frac{3}{2}$	$\frac{1}{2}$
	kinetic	−3.065	−3.051	−2.945
	E_1-E_0	−1.518	−1.474	−1.321
$\mathbf{Q}=(\pi,\pi)$	spin	$\frac{3}{2}$	$\frac{3}{2}$	$\frac{1}{2}$
	kinetic	−3.206	−2.958	−2.769
	E_1-E_0	**−1.658**		
$\mathbf{Q}=(2\pi/5,4\pi/5)$	spin	$\frac{1}{2}$		
	kinetic	**−2.803**		
	E_1-E_0	−1.654		
$\mathbf{Q}=(3\pi/5,\pi/5)$	spin	$\frac{1}{2}$		
	kinetic	−2.720		

TABLE II. Total energies, spins, and kinetic energies of the one-hole lowest states on a 16-site cluster ($J/t=0.25$). The classification is done according to the momentum $\mathbf{Q}$ and the different irreducible representations of the little groups of $\mathbf{Q}$, C_{4v}, C_{2v}, and C_s. The related orbital symmetries are indicated between parenthesis [only valid for $\mathbf{Q}=0$ and $\mathbf{Q}=(\pi,\pi)$]. A question mark (?) means that there are excited states of different spin with the small energy differences.

		$A_1(s)$	$A_2(s')$	$B_1(d_{x^2-y^2})$	$B_2(d_{xy})$	$E(p_x,p_y)$
	E_1-E_0	−1.557	−1.295	**−1.473**	−1.525	−1.452
$\mathbf{Q}=(0,0)$	spin	$\frac{1}{2}$	$\frac{1}{2}$	$\frac{1}{2}$	$\frac{3}{2}$	$\frac{1}{2}$
	kinetic	−3.002	−2.970	**−3.009**	−3.035	−2.908
	E_1-E_0	−1.518	−1.227	−1.434	−1.534	−1.453
$\mathbf{Q}=(\pi,\pi)$	spin	$\frac{3}{2}$	$\frac{3}{2}$	$\frac{1}{2}$	$\frac{3}{2}$	$\frac{1}{2}$
	kinetic	−3.039	−2.980	−3.045	−3.004	−2.937
	E_1-E_0	**−1.894**	−1.190	**−1.473**	−1.434	
$\mathbf{Q}=(\pi,0)$	spin	$\frac{1}{2}$	$\frac{1}{2}$	$\frac{1}{2}$	$\frac{1}{2}$	
	kinetic	**−2.896**	−2.985	**−3.009**	−3.045	
	E_1-E_0	**−1.894**	−1.452			
$\mathbf{Q}=(\pi/2,\pi/2)$	spin	$\frac{1}{2}$	$\frac{1}{2}$			
	kinetic	**−2.896**	−2.922			
	E_1-E_0	−1.776	−1.491			
$\mathbf{Q}=(\pi/2,0)$	spin	$\frac{1}{2}$	$\frac{1}{2}$			
	kinetic	−2.844	−2.970			
	E_1-E_0	−1.700	−1.490			
$\mathbf{Q}=(\pi,\pi/2)$	spin	?	$\frac{3}{2}$			
	kinetic	−2.875	−2.982			

TABLE III. Total energies, spins, and kinetic energies of the one-hole lowest states on a 18-site cluster ($J/t=0.25$). The classification is done according to the momentum $\mathbf{Q}$. Depending on $\mathbf{Q}$ the point groups involved are C_{4v} and C_s.

		$A_1(s)$	$A_2(s')$	$B_1(d_{x^2-y^2})$	$B_2(d_{xy})$	$E(p_x,p_y)$
	E_1-E_0	−1.683	−1.309	−1.378	−1.644	−1.537
$\mathbf{Q}=(0,0)$	spin	$\frac{1}{2}$	$\frac{1}{2}$	$\frac{3}{2}$	$\frac{3}{2}$	$\frac{3}{2}$
	kinetic	−3.150	−3.181	−2.985	−3.081	−3.073
	E_1-E_0	−1.573	−1.284	−1.420	−1.734	−1.534
$\mathbf{Q}=(\pi,\pi)$	spin	$\frac{3}{2}$	$\frac{1}{2}$	$\frac{1}{2}$	$\frac{3}{2}$	$\frac{3}{2}$
	kinetic	−3.091	−3.091	−3.016	−3.149	−3.157
	E_1-E_0	−1.846	−1.640			
$\mathbf{Q}=(2\pi/3,2\pi/3)$	spin	$\frac{3}{2}$	$\frac{1}{2}$			
	kinetic	−3.052	−3.028			
	E_1-E_0	−1.988	−1.553			
$\mathbf{Q}=(\pi/3,\pi/3)$	spin	$\frac{1}{2}$	$\frac{1}{2}$			
	kinetic	−3.074	−2.997			
	E_1-E_0	**−2.004**	−1.585			
$\mathbf{Q}=(2\pi/3,0)$	spin	$\frac{1}{2}$	?			
	kinetic	**−3.035**	−3.119			
	E_1-E_0	−1.954	−1.606			
$\mathbf{Q}=(\pi,\pi/3)$	spin	$\frac{1}{2}$	$\frac{1}{2}$			
	kinetic	−3.036	−3.158			

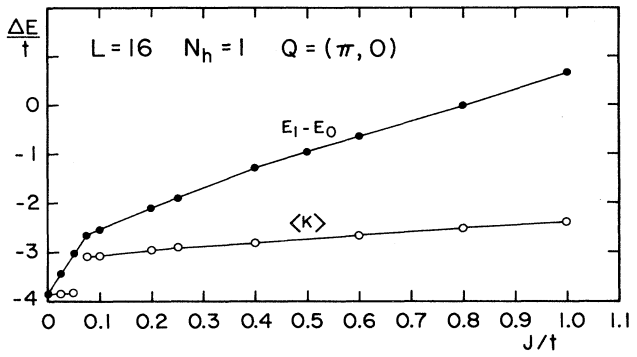

FIG. 1. Energy differences between the one hole and the Heisenberg total energies on a 16-site cluster vs J/t. A discontinuity in the kinetic energy (open circles) is shown at the ferromagnetic transition.

pared to the noninteracting limit ($U=0$). For $L=18$, the two quadruplets of wave vectors inside the FS in the vicinity of $\pm(\pm\pi/2,\pi/2)$ and $(\pi,0),(0,\pi)$ are always very close in energy (within at most $J/10$). Although the degeneracy is exact for 16 sites, it becomes here approximate. The smaller J/t the closer in energy these levels. However, the actual GS momentum location has a crossover around $(J/t)_2=0.2$ from $\sim(\pi/2,\pi/2)$ to $\sim(\pi,0)$ with increasing J/t.

Interesting physical insights can be obtained by splitting Hamiltonian (1) into its two parts. Above $(J/t)_1$ the kinetic energy of the hole (the magnetic energy lost) is an increasing (decreasing) function of J/t. The number of broken bonds, a significant quantity related to the magnetic energy lost by adding one hole, is defined as $[(J/t)_1 \le J/t \le \infty]$

$$\omega=\frac{\sum_{\langle ij\rangle}\langle \mathbf{S}_i\cdot\mathbf{S}_j\rangle-\langle \mathbf{S}_i\cdot\mathbf{S}_j\rangle_0}{|\langle \mathbf{S}_i\cdot\mathbf{S}_j\rangle_0|}\ . \tag{4}$$

The subscript 0 in (4) refers to the Heisenberg model on the same clusters; $\langle \mathbf{S}_i\cdot\mathbf{S}_j\rangle_0=-0.3509,-0.3470$ for $L=16,18$. Before the ferromagnetic transition, our data fit the following behavior [Figs. 2(a) and 2(b)] on the range $(J/t)_1 \le J/t \le 1$;

$$\omega=\omega_0+\omega_1(J/t)^{-\nu}\ ,$$
$$\langle H_K/t\rangle=K_0+K_1(J/t)^{1-\nu}+K_2(J/t)\ . \tag{5}$$

K_0 is the maximum kinetic energy a hole can gain in a $S=\frac{1}{2}$ spin state. We found $\nu\sim0.33$, $\omega_0=1.29$, $\omega_1=4.63$, $K_0=-3.19$, $K_1=0.723$, and $K_2=0.06$ for $L=16$ sites. For $L=18$, we have considered the two nearly degenerate wave vectors (inside the FS). We found $\nu\sim0.12,0.11$, $\omega_0=-2.9,-5.4$, $\omega_1=6.0,8.4$, $K_0=-3.3,-3.4$, $K_1=0.85,2.1$, and $K_2=0.058,-1.1$ for $Q\sim(\pi/2,\pi/2)$ and $Q\sim(\pi,0)$, respectively. The value for K_0 lies within 10% of the Brinkman-Rice (BR) retraceable path approximation estimation, $-3.46(2\sqrt{3})$.[12] The fluctuations of the antiferromagnetic background around the hole are expected to be very important and may explain this small discrepancy. This behavior extrapolated to vanishing J/t (where a transition to the ferromagnetic phase actually appears) would lead to a divergence of ω like in the simple-minded ferromagnetic polaron calculation (where $\nu=\frac{1}{2}$) or in the string calculation which yields $\nu_{\rm Ising}=\frac{1}{3}$.[13] In a finite-size cluster this divergence is cut off below a value of $J/t\sim1/L^{\nu}$. The form (5) for the kinetic terms comes simply from the competition between kinetic energy gain and magnetic lost. It is interesting to note that this kind of polaron effect appears in a continuous $S=\frac{1}{2}$ state. On the other hand, it seems that the spin-flip term ($J_\perp$) in the Hamiltonian will be responsible for a sizable decrease of the exponent ν compared to the value $\nu_{\rm Ising}=\frac{1}{3}$ predicted by the "string" argument[13] or the BR picture applied to the Ising limit.[13] $\langle H_K\rangle$ is discontinuous at $(J/t)_1$, where

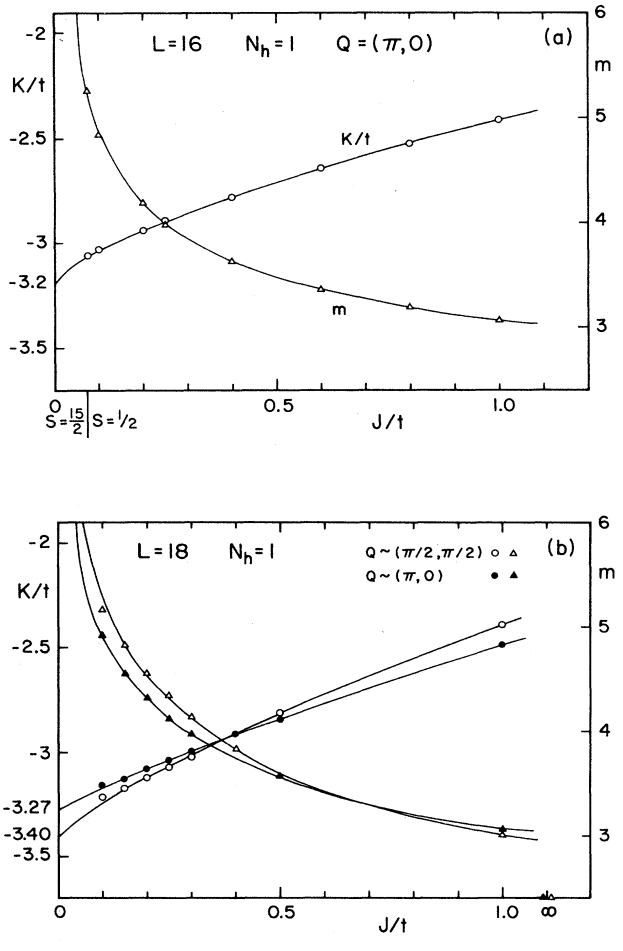

FIG. 2. Magnetic energy loss $m=\sum_{\langle ij\rangle}(\mathbf{S}_i\cdot\mathbf{S}_j-\frac{1}{4}n_in_j)$ and kinetic energy gain of a hole on a 16-site cluster vs J/t. The solid lines correspond to our fit (see text). (a) 16-site cluster. (b) 18-site cluster; the results are shown for the two nonequivalent wave vectors close to the FS.

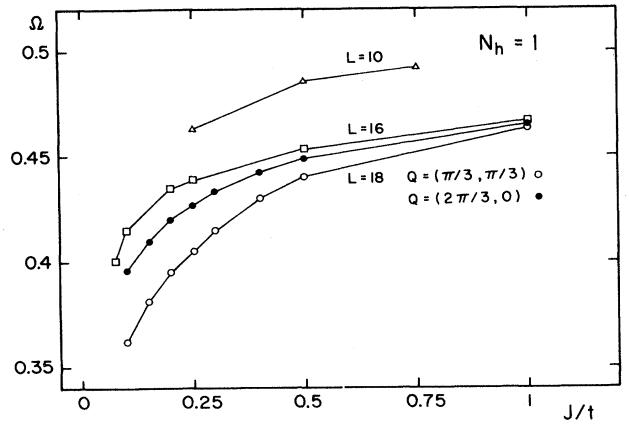

FIG. 3. Staggered magnetization as a function of J/t for one-hole doped clusters in the $S=\frac{1}{2}$ phase.

it drops to a value close to $-4t$ since the hole behaves there as a free particle in a ferromagnetic background. However the ferromagnetic polaron appears only for relatively small J/t. For larger values, our results are consistent with the band narrowing of the hole due to the AF background predicted by the BR picture. On the other hand, in the extreme $J/t\rightarrow\infty$ limit of a static hole, where (5) is no longer valid, the number of broken bonds is slightly smaller than 4, 3.85 and 3.96 for $L=16$ and $L=18$, respectively, which indicates a small increase of the correlations for the 12 bonds connected to the four NN positions to the hole.

We have also studied the behavior with J/t of the staggered magnetization Ω defined by

$$\Omega^2=\left\langle\left[1/L\sum_i(-1)^i\mathbf{S}_i\right]^2\right\rangle . \tag{6}$$

As shown from Fig. 3, the additional hole is first responsible for an overall decrease of Ω compared to the Heisenberg case. Ω has also an interesting behavior as a function of J/t; although it is rather smooth for intermediate values ($J/t\sim0.5$) it is rapidly decreasing when $J/t\rightarrow0$. Although this is closely related to the singularity in ω, this effect is a proof that the hole does not affect correlations between NN only but also at larger distances. On the range $(J/t)_1\leq J/t\leq1$, Ω can be well approximated by a power-law behavior $\Omega\sim(J/t)^\eta$, $\eta=0.06$, and 0.1 for $L=16$ and 18. This may lead to the disappearance of true antiferromagnetic LRO in the thermodynamic limit for a reasonable hole concentration ($\sim6\%$ here).

The distribution of the z component of the spin around the hole $\langle S_i^z n_h(\mathbf{r}_0)\rangle$ shown in Fig. 4 is a relevant physical quantity to study. It couples to a uniform magnetic field and can be indirectly measured by NMR experiments for example. On the whole range of J/t we have considered, this quantity is widely delocalized around the hole. In the large J/t limit, it seems to spread over the sublattice to which the hole does not belong.

C. Two-holes GS properties

Using a similar Lanczos algorithm, we have studied two holes on 10- and 16-site clusters. The energy values and the spin quantum numbers are given in Tables IV and V for an intermediate value $J/t=0.25$.

On the whole range $0\leq J/t\leq\infty$, the GS is found to be a singlet ($S=0$). This is consistent with the fact that the Nagaoka argument does not apply to the system with two holes. For $J=0$, the kinetic energy per hole is found to be -3.0 ($L=10$), -3.339 ($L=16$), larger (in magnitude) than $-(2+\cos k_z+\cos k_y)$ [where (k_x,k_y) is the closest wave vector to the Γ point], which the hole can have in a fully polarized state ($S=S_{\max}$). The behavior of the kinetic and magnetic energies versus J/t is shown in Fig. 5. The wave vector is always found to be uniform ($\mathbf{Q}=0$). However, above a critical value (see later) $\mathbf{Q}=0$ becomes degenerate with $\mathbf{Q}=\pm(2\pi/5,4\pi/5)$ and $\pm(-4\pi/5,2\pi/5)$ and $\mathbf{Q}=(\pi,0)$ and $(0,\pi)$ for $L=10$ and 16, respectively. For $L=16$, this is intrinsically related to the S_4 permutation group on the 2^4 hypercube. For $L=10$, it is also possible to permute two pairs of sites in such a way that the NN distances between all the sites are unchanged. This ambiguity may be lifted by di-

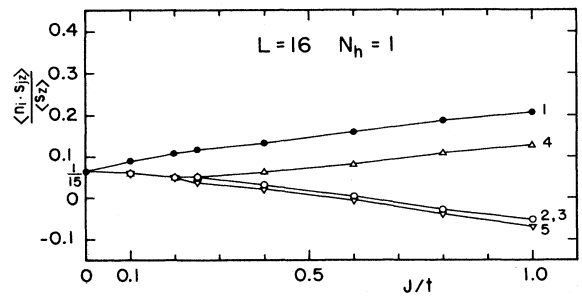

FIG. 4. Distribution of the excess S_z component ($\frac{1}{2}$) of the spin around the hole vs J/t.

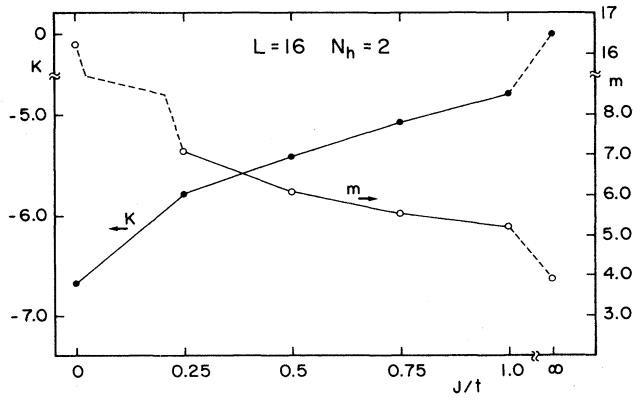

FIG. 5. Magnetic energy loss $m=\sum_{\langle ij\rangle}(\mathbf{S}_i-\mathbf{S}_j-\frac{1}{4}n_in_j)$ and kinetic energy gain of two holes on a 16-site cluster vs J/t.

TABLE IV. Total energies, spins, and kinetic energies of the two-hole lowest states on a 10-site cluster ($J/t=0.25$).

		A_1	B_1	E
	E_2-E_0	−3.566	**−3.652**	−3.504
$\mathbf{Q}=(0,0)$	spin	0	**0**	1
	kinetic	−5.966	**−5.606**	−5.603
	E_2-E_0	−2.902	−3.346	−3.150
$\mathbf{Q}=(\pi,\pi)$	spin	1	1	2
	kinetic	−5.050	−5.291	−5.242
	E_2-E_0	**−3.652**		
$\mathbf{Q}=(2\pi/5,4\pi/5)$	spin	**0**		
	kinetic	**−5.606**		
	E_2-E_0	−3.451		
$\mathbf{Q}=(3\pi/5,\pi/5)$	spin	1		
	kinetic	−5.812		

agonalizing the 18-site cluster with two holes but we do not have the result up to now.

Let us discuss now the GS properties under point group operations. For a uniform state ($\mathbf{Q}=0$) the different irreducible representations can be classified in terms of orbital symmetries s, s', $d_{x^2-y^2}$, d_{xy} and the doublet $[p_x,p_y]$ ($L=16$). However one should notice that for ten sites the reflexions do not exist so that there is only one kind of s or d symmetry. For both sizes we found a crossover between s-type, at small J/t to d-type symmetry at larger J/t. For $L=16$, it is more precisely $s\rightarrow d_{x^2-y^2}$. The critical value lies around $J/t=0.1$–0.25 and 0–0.1 for 10 and 16 sites, respectively. As already mentioned above, this crossover is simultaneous with the momentum transition from a nondegenerate to a degenerate GS.

Hole-hole correlations defined as

$$C(\mathbf{r})=\left\langle \frac{1}{L}\sum_i n_h(\mathbf{r}_i)n_h(\mathbf{r}_i+\mathbf{r})\right\rangle , \tag{7}$$

where $n_h(\mathbf{r}_i)=1-n_i$ have been computed and are reported on Fig. 6. Actually we have performed an average over all possible degenerate GS so that $C(\mathbf{r})$ depends only on the modulus $r=|\mathbf{r}|$.

One can study the tendency of the two holes to bind together by defining the quantity

$$\Delta=(E_2-E_0)-2(E_1-E_0) , \tag{8}$$

where E_2, E_1, and E_0 refer to the two holes, one hole, and Heisenberg GS energies on the same cluster. A negative value of Δ is an indication of an effective attraction although it is not yet clear how Δ will scale with the size. We have plotted Δ versus J/t on Fig. 7. This clearly

TABLE V. Total energies, spins, and kinetic energies of the two-hole lowest states on a 16-site cluster ($J/t=0.25$). See Table II for symmetry classification.

		$A_1(s)$	$A_2(s')$	$B_1(d_{x^2-y^2})$	$B_2(d_{xy})$	$E(p_x,p_y)$
	E_2-E_0	−3.72	−3.55	**−4.000**	−3.42	−3.76
$\mathbf{Q}=(0,0)$	spin	0	0	**0**	0	1
	kinetic	−6.04	−5.68	**−5.78**	−5.84	−5.76
	E_2-E_0	−3.31	−3.66	−3.81	−3.52	−3.81
$\mathbf{Q}=(\pi,\pi)$	spin	1	0	1	0	0
	kinetic	−5.81	−5.87	−5.73	−5.94	−5.61
	E_2-E_0	−3.66	−3.80	**−4.000**	−3.81	
$\mathbf{Q}=(\pi,0)$	spin	1	1	**0**	1	
	kinetic	−5.91	−5.70	**−5.78**	−5.73	
	E_2-E_0	−3.79	−3.81			
$\mathbf{Q}=(\pi/2,\pi/2)$	spin	1	0			
	kinetic	−5.71	−5.62			
	E_2-E_0	−3.73	−3.77			
$\mathbf{Q}=(\pi/2,0)$	spin	0	1			
	kinetic	−5.67	−5.74			
	E_2-E_0	−3.77	−3.73			
$\mathbf{Q}=(\pi,\pi/2)$	spin	1	0			
	kinetic	−5.74	−5.67			

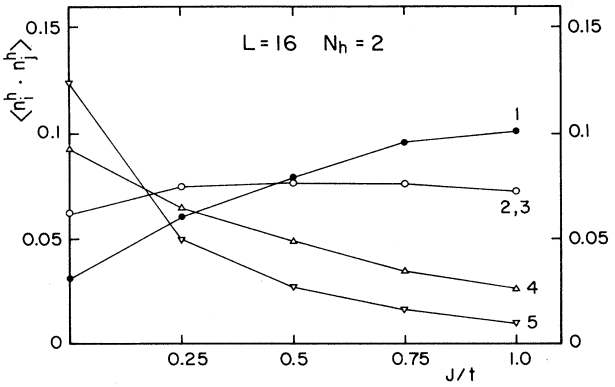

FIG. 6. Hole-hole correlation vs J/t. 1,2, etc. refer to NN, second NN and so on.

shows a net binding roughly proportional to J above a critical value of 0.25 in agreement with Ref. 6.

III. VARIATIONAL RVB STATES

A. General construction

Linear superposition of valence-bond configurations can be simply constructed for infinite systems as well as for finite clusters. Although the RVB wave function gives extremely good results for the Heisenberg model, its validity is still controversial for the doped system. However, since the ground states of the two holes clusters are singlets (even for $J=0$) the RVB is *a priori* a good candidate to describe the GS properties. Besides mean-field theories[14,15] different classes of such wave functions were studied by variational Monte Carlo simulations[16,17] (VMC) or, for the Heisenberg model, by exact diagonalization studies[8,9] or moment calculations.[18] Let us first consider the following complex form of RVB:

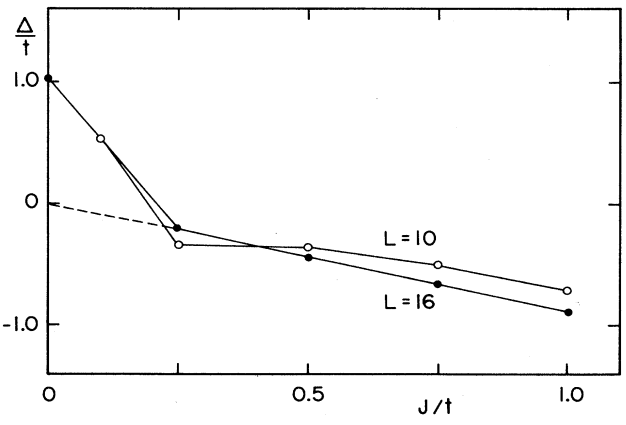

FIG. 7. Two-hole binding energy vs J/t.

$$|\Psi_{\mathrm{RVB}}(\{a_{ij}^0\})\rangle = P_d \left[\sum_{i,j} a(\mathbf{r}_i,\mathbf{r}_j) c_{i\uparrow}^\dagger c_{j\downarrow}^\dagger \right]^{N/2} |0\rangle \ ,$$
$$P_d = \prod_i (1-n_{i\uparrow}n_{i\downarrow}) \ , \tag{9}$$

where $c_{i\sigma}^\dagger$ creates an electron of spin σ at site i, $n_{i\sigma}$ is the particle number operator, $|0\rangle$ the vacuum state, and P_d is the projector on the subspace of no doubly occupied site so that (7) is defined on the same Hilbert space as Hamiltonian (1). N is the actual number of electrons and we will consider the two hole case, $N=L-2$ ($L=10$ and 16).

The factorized form (9) can be expanded and gives a superposition of valence-bond configurations. These are defined by $N/2$ singlet bonds over $L-2=N$ sites in a way that each site (which does not have a hole) belongs to exactly one bond. The $a(\mathbf{r}_i,\mathbf{r}_j)$ describe the probability to find a singlet bond between the lattice sites i and j. They have the variational form $a(\mathbf{r}_i,\mathbf{r}_j) = a_{ij}^0 \exp[i\mathbf{Q}\cdot(\mathbf{r}_i+\mathbf{r}_j)/2]$. We do not set aside *a priori* the possibility of a $\mathbf{Q}=(\pi,0)$ RVB for the $L=16$ cluster where the GS (for sufficiently large values of J/t) is at least threefold degenerate of wave vectors $\mathbf{Q}=0$ or $\mathbf{Q}=(\pi,0)(0,\pi)$ However, as we shall show later, energy calculations will rule out this finite Q RVB against the zero momentum RVB. The singlet pairing amplitudes $a_{ij}^0=a^0(\mathbf{r}_i-\mathbf{r}_j)$ are $N/2$ complex variational parameters which are chosen so as to minimize the energy expectation value. In order to get a singlet state (total spin $S=0$), it is necessary that they are even functions of the position, $a^0(\mathbf{r})=a^0(-\mathbf{r})$. For a given configuration $\{i\uparrow,j\downarrow\}$ characterized by the positions of the up and down spins on the cluster, the corresponding amplitude of (9) is simply given by the determinant of the $N/2\times N/2$ matrix $\{a(\mathbf{r}_{i\uparrow},\mathbf{r}_{j\downarrow})\}$. The correct calculation of the phase factors of the amplitudes arising from the permutations of the fermion operators after expanding (9) is a tedious problem.

First, let us assume that the singlet distribution is chosen to be translational invariant leading to a RVB wave function of $\mathbf{Q}=0$ wave vector (and total spin $S=0$). The remaining symmetries of the trial wave function (under rotation and reflexion) are closely related to the symmetries of the a_{ij}^0 under the same operations. Under $\pi/2$ rotation, $\mathbf{r}_j \to \tilde{\mathbf{r}}_{ij}$, and reflections (along x or y), $\mathbf{r}_{ij} \to \hat{\mathbf{r}}_{ij}$, the latter tranform as

$$a_{ij}^0 \to \tilde{a}_{ij} = a^0(\tilde{\mathbf{r}}_{ij}) = -(a_{ij}^0)^* \ ,$$
$$a_{ij}^0 \to \bar{a}_{ij} = a^0(\bar{\mathbf{r}}_{ij}) \ , \tag{10}$$

respectively. We have assumed "$s+id$" symmetry under rotation but no special constraint under reflexion. That means that $|\Psi_{\mathrm{RVB}}\rangle$ breaks both symmetries and expands over several space-group representations,

$$|\Psi_{\mathrm{RVB}}(\{a_{ij}^0\})\rangle = \sum_{R,\gamma} h_{R,\gamma} |\Psi_R^\gamma\rangle \ . \tag{11}$$

The index R corresponds (for a 16-site cluster) to the s, s', $d_{x^2-y^2}$, and d_{xy} representations. (s' states are antisymmetric with respect to reflections.) The doubly degen-

erate representation (E) is not involved since the $a^0(\mathbf{r})$ are even functions of $\mathbf{r}$. It should be noted that these irreducible representations correspond to the symmetries of the wave functions, not of the pairing correlation functions. By transforming the set of a_{ij}^0 under each point group operation (see Eq. 10) it then becomes possible to define four degenerate RVB states (two pairs of complex conjugate states) which have nonzero off-diagonal Hamiltonian matrix elements,

$$|\Psi_{\mathrm{RVB}}(\{a_{ij}^0\})\rangle,\quad |\Psi_{\mathrm{RVB}}^*(\{a_{ij}^0\})\rangle\ ,$$
$$|\Psi_{\mathrm{RVB}}(\{\bar{a}_{ij}\})\rangle,\quad |\Psi_{\mathrm{RVB}}^*(\{\bar{a}_{ij}\})\rangle\ . \tag{12}$$

A linear superposition of those restores the square lattice symmetries and can lead to a lowering of the energy expectation value. This is performed as follows ($L=16$):

$$\begin{aligned}
|\Psi_{d_{x^2-y^2}}\rangle &= \mathrm{Re}[|\Psi_{\mathrm{RVB}}(\{a_{ij}^0\})\rangle + |\Psi_{\mathrm{RVB}}(\{\bar{a}_{ij}\})\rangle]\ ,\\
|\Psi_{d_{xy}}\rangle &= \mathrm{Re}[|\Psi_{\mathrm{RVB}}(\{a_{ij}^0\})\rangle - |\Psi_{\mathrm{RVB}}(\{\bar{a}_{ij}\})\rangle]\ ,\\
|\Psi_{s}\rangle &= \mathrm{Im}[|\Psi_{\mathrm{RVB}}(\{a_{ij}^0\})\rangle + |\Psi_{\mathrm{RVB}}(\{\bar{a}_{ij}\})\rangle]\ ,\\
|\Psi_{s'}\rangle &= \mathrm{Im}[|\Psi_{\mathrm{RVB}}(\{a_{ij}^0\})\rangle - |\Psi_{\mathrm{RVB}}(\{\bar{a}_{ij}\})\rangle]\ .
\end{aligned} \tag{13}$$

One should notice that the 10-site cluster is not invariant under reflections. Consequently there is only one s-type and d-type space-group representation (for $\mathbf{Q}=0$). The corresponding RVB are simply obtained by taking the real and imaginary part of (9).

The assumption (10) is a generalization in the doped system of the "flux phase" RVB for the Heisenberg model defined by NN singlet amplitudes equal to 1 or i along x and y, respectively. However, one should mention first that the flux phase on the Heisenberg lattice does not break the rotational symmetry since the number of vertical bonds is even leading to a real wave function (on a $4n+4$ sites cluster). This is no longer true if one adds two holes on the lattice so that the correct symmetry has to be restored by taking the real or the imaginary part. Secondly, we would like to point out that, in order to increase the kinetic energy, longer bonds are to be now included. Indeed, the kinetic term of (1) connects A—A to A—B bonds (where A and B refer to the two sublattices). A wave function (9) containing only one kinds of bond is doomed to have zero kinetic expectation value. This is not inconsistent with the moments calculation of Lederer and Takahashi[18] of the hole kinetic energy in a "NN RVB": they compute the density of states in a limit where all states are incoherent and eigenstates of the momentum operator are spread evenly over the hole band. Thirdly, it should be stressed that the above symmetry requirements are necessary only for a finite system. However, in the thermodynamic limit, the possibility of rotational symmetry breaking cannot be ruled out *a priori* and a flux phase state of the class (9) with $s+id$ amplitudes may become the best variational candidate. This requires that no nonzero Hamiltonian matrix elements are connecting the four degenerate states (12). This necessary condition is unfortunately violated on finite clusters.

Let us now briefly describe how to construct the $\mathbf{Q}=(\pi,0)$ RVB state ($L=16$). The symmetries that leave the $\mathbf{Q}$ vector invariant are the π rotation and the x reflection leading to the following transformations of the singlet amplitudes:

$$\begin{aligned}
&a(\mathbf{r}_i,\mathbf{r}_j)\rightarrow a(\mathbf{r}_i,\mathbf{r}_j)^*\ ,\\
&a(\mathbf{r}_i,\mathbf{r}_j)\rightarrow \bar{a}_{ij}\exp[i\mathbf{Q}\cdot(\mathbf{r}_i+\mathbf{r}_j)/2]\ ,
\end{aligned} \tag{14}$$

where we have assumed the a_{ij}^0 to have real $s+d$ symmetry. It is then straightforward to see that the symmetry of the exact GS of finite momentum (for $J\geq J_C$) can be achieved by

$$|\Psi(\mathbf{Q}=(\pi,0),B_1)\rangle = \mathrm{Im}[|\Psi_{\mathrm{RVB}}(\{a_{ij}^0\})\rangle + |\Psi_{\mathrm{RVB}}(\{\bar{a}_{ij}\})\rangle]\ . \tag{15}$$

B. Results

The variational form (9) includes the so-called projected BCS wave function,[15,16] simply obtained by the following Fourier transform of the a_{ij}:

$$a_{\mathbf{k}}=\frac{\Delta_{\mathbf{k}}}{\xi_{\mathbf{k}}(\xi_{\mathbf{k}}^2+\Delta_{\mathbf{k}}^2)^{1/2}}\ , \tag{16}$$

where $\xi_{\mathbf{k}}=-2(\cos k_x+\cos k_y)-\mu$ and $\Delta_{\mathbf{k}}=\Delta(\cos k_x-\cos k_y)$ (d wave), $\Delta_k=\Delta(\cos k_x+\cos k_y)-\mu$ (s wave). μ and Δ are taken as variational parameters. The motivation for studying more complicated wave functions than (16) is due to the fact that (16) is improper to describe properly our finite-size systems; the overlap of the d wave $\langle\Psi_{\mathrm{BCS}}|\Psi_{\mathrm{exact}}(d_{x^2-y^2})\rangle$ drops from 0.903 for $L=10$ to 0.04 for $L=16$ ($J/t=0.25$). This may be related to the high degeneracy of the Fermi sea for two holes. However let us mention the results obtained for $L=10$ and $J/t=0.25$; for the d wave (s wave) the kinetic energy per hole and the expectation value of the magnetic term of (2) are $-2.4t$ ($-2.215t$) and $6.7J$ ($7.8J$), respectively. The overlap of the projected BCS with the exact state of corresponding symmetry is 0.903 (0.865).

The variational parameters $a_{ij}^0=|a_{ij}^0|\exp i\phi_{ij}$ have been optimized for different values of J/t for both Ψ_s and $\Psi_{d_{x^2-y^2}}$ (or Ψ_d for $L=10$). Their amplitudes $|a_{ij}^0|$ are found to be smooth functions of the distance between i and j and their phases ϕ_{ij} are mostly distributed around $\pi/6$ and $5\pi/6$. As an example let us assume $L=16$ and $J/t=0.25$; the $d_{x^2-y^2}$ (s) RVB amplitudes $|a_{ij}^0|$ and phases ϕ_{ij} corresponding to the distances (1,0), (1,1), (2,0), (2,1), and (2,2) are approximately 3.0 (3.4), 0.93 (0.53), 5.2 (5.0), 2.3 (1.6), and 1 (1) and $\pi/6$ ($\pi/5$), $\pi/2$ ($\pi/2$), $\pi/5$ ($\pi/5$), $\pi/4$ ($\pi/5$), and $\pi/2$ ($\pi/2$), respectively. The behavior of the kinetic and magnetic expectation values with J/t is similar to their behaviors in the actual GS (see Fig. 5) although the magnitudes of the changes in the range $0\leq J/t\leq 1$ are significantly smaller. While the hole in the s-RVB gains more kinetic energy than in the d-RVB, it costs more magnetic energy. Therefore there is a smooth crossover between s type to d type with in-

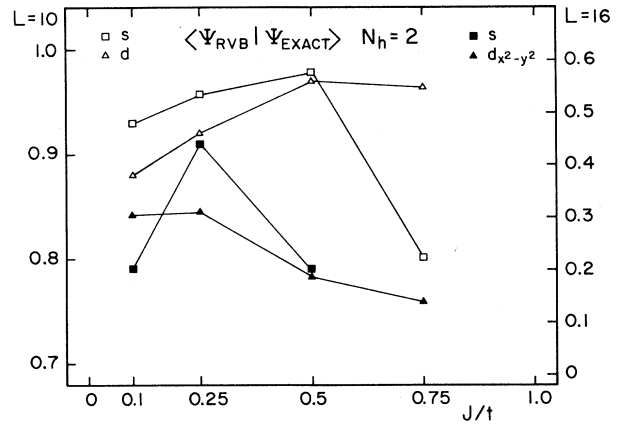

FIG. 8. Overlaps $\langle \Psi_{\mathrm{RVB}} | \Psi_{\mathrm{exact}} \rangle$ between the RVB state and the lowest exact state of the same symmetries under rotations (and reflexions for $L=16$). The actual GS has alternatively s and d symmetry when J/t increases.

creasing J/t. This is located around $J/t=0.25$ and $J/t=0.75$ for $L=10$ and 16.

Let us now consider the $J=0$ limit; the two holes in the 16-site cluster can gain $\langle H_K \rangle = -2.79$ and -2.77 per hole in the s- and d-type RVB, respectively, in agreement with results by Lederer and Takahashi.[18] Although this is above the energy gain (-3.0) in a ferromagnetically polarized state, we expect the spin liquid state to account properly for the spin fluctuations as soon as a finite value of J/t is assumed. Indeed the overlaps of Ψ_s and $\Psi_{d_{x^2-y^2}}$ with the corresponding lowest states of the same symmetry show maxima at intermediate values of J/t as plotted in Fig. 8. For $J/t=0.25$, $L=16$, the relative kinetic energy gains (magnetic losses) differ from the exact states of only -9.5% ($+26\%$) and -8.9% (-0.8%) for $d_{x^2-y^2}$ and s-RVB, respectively.

IV. CONCLUSION

We have studied the GS of the t-J model for one hole on 10, 16, and 18 sites and two holes on 10 and 16 sites. New physical insights can be obtained by considering separately the kinetic energy and magnetic energy as a function of J/t. The number of bonds broken by a single hole (staggered magnetization) is increasing (decreasing) with a power-law behavior as $J/t \to 0$.

The GS in the case of two holes is a singlet for all range of J/t. Therefore, contrary to the one-hole case, the fully polarized ferromagnetic state is unstable against the singlet state even in the extreme $J=0$ limit. The symmetry of the GS is found to change with J/t; for small J/t the GS is $\mathbf{Q}=0$ and symmetric with respect to point group operations. For J/t larger than the critical value, the GS is antisymmetric with respect to $\pi/2$ rotation and becomes degenerate to $\mathbf{Q}\neq 0$ states. This degeneracy is due to the specific symmetries of $L=10$ and 16 sites with periodic boundary conditions. In order to determine nonambiguously the GS momentum large size calculations are necessary. The binding energy of two holes is roughly proportional to J.

We calculated the variational RVB state with two holes. As the exact GS, the symmetry of the lowest energy RVB state is also shown to change from s wave to d wave. The overlap of the RVB and the exact state becomes maximum around $J/t \sim 0.25$–0.5.

After this work was completed we received various preprints addresing the question of the stability of the ferromagnetic state in the one-bond Hubbard model.[19]

ACKNOWLEDGMENTS

We would like to thank T. M. Rice for numerous stimulating discussions and comments. We also thank P. Lederer for clarifying discussions concerning the kinetic energy of a hole in an RVB state and M. Sigrist for helpful comments on space-group theory. The numerical calculations reported in this paper were done on the Cray-XMP/28 at the Eidgenössische Technische Hochschule Zürich (ETHZ). The Swiss National Fond is acknowledged for financial support.

*On leave from the Institute for Solid State Physics, The University of Tokyo, 7-22-1 Roppongi Minato-ku, Tokyo 106, Japan.

[1] P. W. Anderson, Science **235**, 1196 (1987).
[2] F. C. Zhang and T. M. Rice, Phys. Rev. B **37**, 3759 (1988).
[3] S. Tang and J. E. Hirsch, Phys. Rev. B **39**, 4548 (1989).
[4] J. P. Reger and A. P. Young, Phys. Rev B **37**, 5978 (1988).
[5] E. Dagotto, J. R. Schrieffer, A. Moreo, and T. Barnes (unpublished).
[6] J. Bonča, P. Prelovšek, and I. Sega, Phys. Rev. B **39**, 7074 (1989).
[7] J. A. Riera and A. P. Young, Phys. Rev. B **39**, 9697 (1989).
[8] M. Inoue, T. Chikyu, X. Hu, and M. Suzuki, J. Phys. Soc. Jpn. **57**, 3733 (1988).
[9] D. Poilblanc, Phys. Rev. B **39**, 140 (1989).
[10] E. Dagotto and A. Moreo, Phys. Rev. D **31**, 865 (1985).
[11] While this work was completed we received a copy of unpublished work from M. Ogata and H. Shiba. We thank them for discussing their results with us in order to reach a common agreement on the 10-site cluster.
[12] W. F. Brinkman and T. M. Rice, Phys. Rev. B **2**, 1324 (1970).
[13] N. Bulaevskii, É. L. Nagaev and D. I. Khomskiĭ, Zh. Eksp. Teor. Fiz. **54**, 1562 (1968) [Sov. Phys.—JETP **27**, 836 (1968)]; B. Shraiman and E. Siggia, Phys. Rev. Lett. **60**, 740 (1988).
[14] Y. Suzumura, Y. Hasegawa, and H. Fukuyama, J. Phys. Soc. Jpn. **57**, 2768 (1988).
[15] F. C. Zhang, C. Gros, T. M. Rice, and H. Shiba, Supercond. Sci. Technol. **1**, 36 (1988).
[16] C. Gros, Phys. Rev. B **38**, 931 (1988).
[17] H. Yokoyama and H. Shiba, J. Phys. Soc. Jpn. **57**, 2482 (1988).
[18] P. Lederer and Y. Takahashi, Z. Phys. B **71**, 415 (1988).
[19] J. A. Riera and A. P. Young (unpublished); Y. Fang, A. R. Ruckenstein, E. Dagotto, and S. Schmitt-Rink (unpublished); B. S. Shastry, H. R. Krishnamurthy, and P. W. Anderson (unpublished).